



AFRL-SA-WP-TR-2013-0021

Noninvasive Intracranial Pressure Monitoring Using Advanced Machine Learning Techniques



**Peter Hu, PhD; Shiming Yang, PhD; Hegang Chen, PhD;
Lynn Stansbury, MD; Catriona Miller, PhD; Katharine
Colton; Kostas Kalpakis, PhD; Col Raymond Fang, MD;
Deborah M. Stein, MD, MPH, FACS**



November 2013

**Final Report
for August 2012 to August 2013**

**Distribution A: Approved for public
release; distribution is unlimited.
Case Number: 88ABW-2014-1766,
17 Apr 2014**

**Air Force Research Laboratory
711th Human Performance Wing
School of Aerospace Medicine
Air Force Expeditionary Medical Skills Inst
C-STARS Baltimore
2510 Fifth St.
Wright-Patterson AFB, OH 45433-7913**

NOTICE AND SIGNATURE PAGE

Using Government drawings, specifications, or other data included in this document for any purpose other than Government procurement does not in any way obligate the U.S. Government. The fact that the Government formulated or supplied the drawings, specifications, or other data does not license the holder or any other person or corporation or convey any rights or permission to manufacture, use, or sell any patented invention that may relate to them.

Qualified requestors may obtain copies of this report from the Defense Technical Information Center (DTIC) (<http://www.dtic.mil>).

AFRL-SA-WP-TR-2013-0021 HAS BEEN REVIEWED AND IS APPROVED FOR PUBLICATION IN ACCORDANCE WITH ASSIGNED DISTRIBUTION STATEMENT.

//SIGNATURE//

Col Raymond Fang, USAF, MC, FS
Chief, C-STARS Baltimore

//SIGNATURE//

Col Benjamin A. Harris, USAF, MC, SFS
Chair, AF Expeditionary Medical Skills Inst

This report is published in the interest of scientific and technical information exchange, and its publication does not constitute the Government's approval or disapproval of its ideas or findings.

REPORT DOCUMENTATION PAGE			<i>Form Approved</i> <i>OMB No. 0704-0188</i>		
Public reporting burden for this collection of information is estimated to average 1 hour per response, including the time for reviewing instructions, searching existing data sources, gathering and maintaining the data needed, and completing and reviewing this collection of information. Send comments regarding this burden estimate or any other aspect of this collection of information, including suggestions for reducing this burden to Department of Defense, Washington Headquarters Services, Directorate for Information Operations and Reports (0704-0188), 1215 Jefferson Davis Highway, Suite 1204, Arlington, VA 22202-4302. Respondents should be aware that notwithstanding any other provision of law, no person shall be subject to any penalty for failing to comply with a collection of information if it does not display a currently valid OMB control number. PLEASE DO NOT RETURN YOUR FORM TO THE ABOVE ADDRESS.					
1. REPORT DATE (DD-MM-YYYY) 1 Nov 2013		2. REPORT TYPE Final Technical Report		3. DATES COVERED (From – To) August 2012 – August 2013	
4. TITLE AND SUBTITLE Noninvasive Intracranial Pressure Monitoring Using Advanced Machine Learning Techniques			5a. CONTRACT NUMBER FA8650-11-2-6142		
			5b. GRANT NUMBER		
			5c. PROGRAM ELEMENT NUMBER		
6. AUTHOR(S) Peter Hu, PhD; Shiming Yang, PhD; Hegang Chen, PhD; Lynn Stansbury, MD; Catriona Miller, PhD; Katharine Colton; Konstantinos Kalpakis, PhD; Col Raymond Fang, MD; Deborah M. Stein, MD, MPH, FACS			5d. PROJECT NUMBER		
			5e. TASK NUMBER		
			5f. WORK UNIT NUMBER		
7. PERFORMING ORGANIZATION NAME(S) AND ADDRESS(ES) USAF School of Aerospace Medicine Air Force Expeditionary Medical Skills Institute C-STARS Baltimore 2510 Fifth St. Wright-Patterson AFB, OH 45433-7913			8. PERFORMING ORGANIZATION REPORT NUMBER AFRL-SA-WP-TR-2013-0021		
9. SPONSORING / MONITORING AGENCY NAME(S) AND ADDRESS(ES)			10. SPONSORING/MONITOR'S ACRONYM(S)		
			11. SPONSOR/MONITOR'S REPORT NUMBER(S)		
12. DISTRIBUTION / AVAILABILITY STATEMENT Distribution A: Approved for public release; distribution is unlimited. Case Number: 88ABW-2014-1766, 17 Apr 2014					
13. SUPPLEMENTARY NOTES					
14. ABSTRACT This project explored the use of advanced machine learning techniques to noninvasively estimate real-time intracranial pressure (ICP) in traumatic brain injury patients from continuous electronic physiological monitoring data. We hypothesized that advanced machine learning techniques could process and analyze electronic vital signs data collected noninvasively and, when correlated with central nervous system-invasive ICP monitoring data, could provide a valid analytic platform for the noninvasive monitoring of ICP for defined periods and clinical needs. We developed a machine learning algorithm that, using noninvasive vital signs features alone, could estimate the current ICP of a patient with an accuracy of ± 4.6 mmHg. We further developed algorithms that are capable of predicting patient future ICP with ± 1.5 mmHg 5 minutes into the future and ± 5 mmHg standard deviation 2 hours into the future using the continuous recordings of heart rate, systolic blood pressure, mean arterial pressure, and ICP. Realization of this analytic platform will support translation of this work into robust, field-ready clinical instrumentation that permits high-quality ICP monitoring in austere care environments not suitable for central nervous system-invasive ICP monitoring.					
15. SUBJECT TERMS Advanced machine learning techniques, intracranial pressure, vital signs, monitoring, noninvasive monitoring					
16. SECURITY CLASSIFICATION OF:			17. LIMITATION OF ABSTRACT SAR	18. NUMBER OF PAGES 30	19a. NAME OF RESPONSIBLE PERSON Col Raymond Fang
a. REPORT U	b. ABSTRACT U	c. THIS PAGE U			19b. TELEPHONE NUMBER (include area code)

This page intentionally left blank.

TABLE OF CONTENTS

Section	Page
LIST OF FIGURES	iii
1.0 EXECUTIVE SUMMARY	1
2.0 INTRODUCTION	2
3.0 BACKGROUND	3
3.1 Trauma Epidemiology	3
3.2 Clinical Application and Pitfalls.....	3
3.3 Preliminary Studies.....	3
4.0 METHODS	4
4.1 Data Sources: Patient Selection	4
4.2 Data Sources: Patient Records.....	5
4.3 High-Resolution Automated Data Collection.....	5
4.4 Data Pre-Processing.....	5
4.5 Time Series Analysis of ICP	6
4.5.1 Auto-Correlation Study.....	6
4.5.2 Cross-Correlation Study.....	7
4.5.3 Vital Signs Variable Dependency Test.....	7
4.6 Estimate ICP Via Low-Rank Matrix Completion.....	8
4.7 ICP Prediction Via Nearest Neighbor Regression.....	10
4.7.1 Predictions with Past ICP Measurement.....	10
4.7.2 Predictions with Noninvasive Vital Signs Measurement.....	11
4.8 Evaluation of Drug Treatment and ICP Change.....	11
5.0 RESULTS	12
5.1 Time Series Analysis	12
5.2 Hankel Matrix Completion	12
5.3 Prediction with Nearest Neighbor Regression.....	13
5.4 Drug Treatment and Its Impact on ICP.....	16

TABLE OF CONTENTS (concluded)

Section	Page
6.0 DISCUSSION.....	18
7.0 CONCLUSIONS.....	19
7.1 Immediate Support.....	19
7.2 Cost and Ease of Use	19
7.3 Limitations	20
8.0 REFERENCES	20
LIST OF ABBREVIATIONS AND ACRONYMS	22

LIST OF FIGURES

Figure	Page
1 Real-Time Bedside and Telemetric Critical Care Monitoring Display	4
2 Auto-Correlation Function with Respect to Different Lags for One Patient’s ICP.....	6
3 Jitter Plot of 113 Patients’ ICP Auto-Correlation, with Maximum Lag of 2 h (24 evaluation time points with 5 min each).....	7
4 Cross-Correlation Function with Respect to Different Lags for One Patient’s ICP and HR.....	7
5 Pairwise Relationships of VS, Measured by MIC and Pearson’s (Linear) Correlation Coefficient	8
6 Example Hankel Matrix for a Sequence of $m=3$ VS Using a Sliding Window of Size $w=7$ ($k=2$).....	9
7 Illustration of Searching Nearest Neighbors Given the Current System State of a New Patient.....	10
8 Scatter Plot of Performance of Data Imputation Methods.....	13
9 Bland-Altman Plots of Performance of Data Imputation Methods	14
10 Performance of Comparison of Prediction for Different Prediction Horizons (5 min, 1 h, and 2 h) of the NNR Using Past ICP.....	15
11 1.96 SD and Bias of ICP Predictions of NNR, Regression Tree, and Most Recent ICP Carry-On.....	16
12 PTD20 in the Hours Before, During, and After Treatment Administration for Different Types of Drugs	17
13 PTI20 in the Hours Before, During, and After Treatment Administration for Different Types of Drugs	18

This page intentionally left blank.

1.0 EXECUTIVE SUMMARY

The vast amounts of high-quality continuous electronic data garnered by modern physiologic monitoring systems have the potential to provide an unprecedented view of dynamic physiologic response to injury, illness, and intervention. We hypothesized that advanced machine learning techniques could process and analyze electronic vital signs (VS) data collected noninvasively and, when correlated with invasive intracranial pressure (ICP) monitoring data, provide a valid analytic platform for the noninvasive monitoring of ICP for defined periods and clinical needs. The primary aim of this project was to demonstrate the correlation between ICP data derived from invasive systems with VS data from non-central nervous system-invasive systems in the prediction of immediately subsequent periods of ICP using advanced machine learning techniques. To accomplish this aim, we had three objectives:

1. Establish a validated patient database and pool of testing data from the continuous, automated electronic monitoring network in our neurotrauma critical care units and identify, using multivariate, nonlinear regression methods, those time-and-sequence segments of continuous electronic VS data, so-called features, of potential utility in prediction models.
2. Using the subset of critical features identified in the above work and three well-described structured machine learning methods—decision tree, support vector machines, and entropy—construct machine learning models that correlate previous periods of invasively derived ICP data and previous periods of noninvasively derived VS data with immediately subsequent periods of invasively derived ICP.
3. Cross-validate the above results using three established techniques—leave-one-out, k-fold, and receiver operating characteristics area under the curve analysis—to estimate the prediction error of each model without overfitting the model

Between 2008 and 2010, there were 207 cases of traumatic brain injury patients admitted to the R Adams Cowley Shock Trauma Center in which continuous ICP monitors were placed and continuous electronic physiologic data were recorded; 191 of these patients were older than 18 years of age and eligible for this study. There are more than 50 types of vital signs routinely collected on all patients admitted to the Shock Trauma Center neurotrauma critical care units, including continuous ICP, heart rate, systolic blood pressure, and end tidal carbon dioxide. Additional data collected included patient demographics, injury types, drug treatments, and outcome data.

Because of the large size and complexity of the patient dataset, the dataset was pre-processed to remove noise and to explore the nature of the dataset prior to building estimation or prediction models. First, the dataset was refined by removing outliers and highly noisy ICP segments. With the remaining high-quality patient dataset, we applied various time series methods to study the predictability of ICP and its correlation with other noninvasive vital signs. Next, we developed a novel approach to real-time estimate ICP levels in incomplete datasets with gaps of missing values from the stream of continuous physiological electronic monitoring data by constructing sequences of Hankel matrices from VS data streams and utilizing the low-rank matrix completion method from compressive sensing to estimate ICP. Our approach substantially outperformed other popular fill-in methods, such as k-nearest neighbors and expectations maximization.

We also developed methods for ICP estimation and near-term ICP prediction by training regression models using VS features for given time durations. Our regression model of minimally invasive ICP monitoring predicts ICP in clinically useful timeframes and may support development of noninvasive and/or minimally invasive ICP monitoring systems, earlier intervention strategies, and better patient outcomes. We developed a machine learning algorithm that, using noninvasive VS features alone, could estimate the current ICP of a patient with an accuracy of ± 4.6 mmHg. We further developed algorithms that are capable of predicting patient future ICP within ± 1.5 mmHg 5 minutes into the future and ± 5 mmHg standard deviation 2 hours into the future using the current continuous recordings of heart rate, systolic blood pressure, mean arterial pressure, and ICP.

Although our estimation and prediction results are encouraging, the prediction accuracy was found to decrease as the prediction horizon extends. A major contributor to the reduced prediction capability of our regression models is the clinical care of the patient, as many clinical interventions and treatments occur that are not adjusted for in the regression models. To address this, we added drug treatment variables to our regression models to improve the accuracy of estimation of ICP. Ninety-eight patients with a collective 664 treatment instances of hypertonic saline, mannitol, barbiturates, propofol, or fentanyl were identified and characterized to study whether intervention information, such as drug treatment, could be included into the estimation models for improving accuracy.

2.0 INTRODUCTION

Combat-related TBI is an important cause of death and persistent disability in the current conflicts [1-3]. Estimates suggest that approximately 20% of all military personnel serving in the current conflicts in the Middle East have suffered some form of traumatic brain injury (TBI), and recent calls for combat casualty care research have specifically targeted advancing TBI care at all echelons of care. Analysis of U.S. military deaths occurring after arrival at a medical facility found that 9% of potentially survivable and 83% of non-survivable “died of wounds” combat deaths were due to combat-related TBI. Among those who survive the initial trauma, additional post-injury secondary physiologic insults begin to accumulate almost immediately, chiefly manifested as brain swelling or intracranial hypertension (ICH), which has a high correlation with poor outcome. Management of severe TBI aims to mitigate secondary insults, and most interventions are directed at controlling intracranial pressure (ICP) and preventing ICH. The current gold standard of treatment involves direct measurement of ICP and ICH, which is invasive and associated with bleeding, infection, and misplacement; requires neurosurgical expertise and an advanced facility; and is not suitable for deployment in austere environments. For these reasons, identification of robust, accurate, reliable, and noninvasive methods for monitoring ICP and secondary injury is a high priority.

Casualties with severe TBI (Glasgow Coma Scale—GCS—8 or less) are particularly vulnerable to the stressors of long-distance air evacuation [4,5], and evacuation itself is not without specific risks for additive injury. Having valid, reliable prognostic information on casualties within the first 12 hours after severe TBI will help optimize triage and evacuation times and improve long-term outcomes for these patients.

3.0 BACKGROUND

3.1 Trauma Epidemiology

Traumatic brain injury is the most common cause of emergency care admission and of trauma-related death in the U.S. civilian population [6] and a major cause of death and disability in combat casualties [7]. For TBI patients, ICP, the pressure measured inside of the closed box of the skull, is of special importance [8]. Even relatively brief periods of elevated ICP are associated with adverse outcomes, and marked elevation of ICP or elevation unresponsive to medications may require risky life-saving surgery. Because of the highly invasive and hazardous nature of direct ICP monitoring and because the management of ICP is a central focus of neurotrauma critical care [9], much research has focused on the development of early-warning decision assist systems that could maximize the potential for timely therapeutic interventions to improve long-term clinical outcomes by estimation and prediction of ICP.

3.2 Clinical Application and Pitfalls

Three clinical application scenarios have been identified that would greatly benefit from noninvasive ICP estimation and ICP prediction based on previous ICP measurements:

1. In austere environments, such as warzones, natural disaster areas, or rural areas, invasive ICP monitoring can be difficult or impossible.
2. Even in patients with invasive ICP monitors installed, various technical complications leading to interruption of ICP measurement are inevitable, such as the limitations of intraventricular catheters capable of ICP measurement or cerebrospinal fluid drainage requiring removal to prevent infection or to allow computed tomography scan.
3. If clinicians had the ability to predict near-future ICP trends, they could initiate timely therapeutic interventions to limit or even prevent secondary injury.

In applying advanced machine learning techniques to continuous electronic physiological monitoring data for the real-time estimation and near-future prediction of ICP, there are two potential pitfalls. First, our patient dataset may be limited due to the technical challenges and sporadic nature of continuous monitoring data, which could limit our ability to build specific models. Second, due to the complexity of the human brain and our incomplete understanding of TBI physiology, we may have limited ability to describe and interpret the interrelationship of ICP with other vital signs (VS). In the following study, we seek to develop a machine learning framework designed to address both potential pitfalls.

3.3 Preliminary Studies

The study team previously demonstrated the superiority of automated VS data collection and processing systems compared to manual VS recording in providing data on patients with severe TBI and the power of calculating a pressure-times-time “dose” (PTD) of ICP and cerebral perfusion pressure (CPP) [8,10]. Using receiver operating characteristic techniques, prognostic algorithms were developed correlating VS-related features derived from routine neurotrauma critical care unit (NTCCU) electronic monitoring with 30-day mortality and Glasgow Outcome

Score-Extended [11] scores at 3 and 6 months. These algorithms were then incorporated into real-time graphic displays of ongoing calculations of Shock Index [SI=systolic blood pressure (SBP)/heart rate (HR)] and Brain Trauma Index (BTI=[CPP/ICP]*time [12]. This prototype patient monitoring video display system is now deployed on a translational basis throughout the R Adams Cowley Shock Trauma Center (STC) in Baltimore, MD (Figure 1).

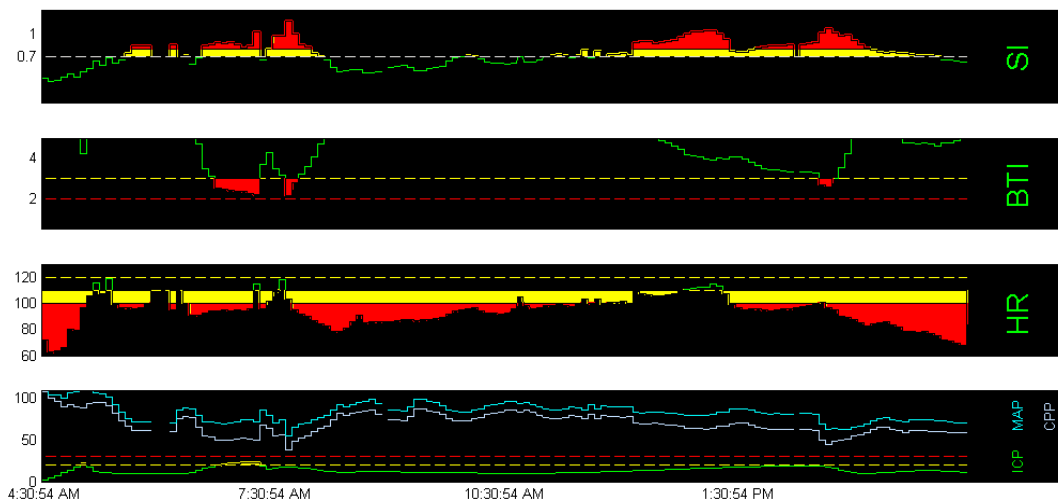


Figure 1. Real-Time Bedside and Telemetric Critical Care Monitoring Display

The BTI graph, shown in the second row from the top in Figure 1, allows for the tracking and visual display of head injury status. Data point clusters under the dotted red line (ICP<20 mmHg and CPP>60 mmHg) are associated with the best outcomes; points between the red and yellow lines correlate with relatively poor outcomes, while the poorest outcomes are seen when data points cluster above the yellow line (ICP≥20 mmHg and CPP<60 mmHg). This display allows clinicians to track and monitor shifts in patients' status over the previous 12 and 24 hours in a single real-time display, linked to predicted outcome rather than just conventional single-parameter threshold readouts. As well as the two indices noted, SI and BTI, VS thresholds of interest in this work were SBP, mean arterial pressure (MAP), HR, ICP, CPP, and oxygen saturation (SpO₂).

4.0 METHODS

4.1 Data Sources: Patient Selection

This work was undertaken as part of the protocol approved by the University of Maryland School of Medicine Human Research Protections Office and the Air Force Research Laboratory's Institutional Review Board for intensive monitoring after severe TBI. Included were adult patients (older than 17 years) admitted to the STC with GCS <9 and a clinically determined requirement for ICP monitoring. The nature of these patients' injuries precluded personal informed consent; therefore, informed consent was secured from a legally authorized representative prior to study inclusion and from the patient as soon as and if that became

possible. Patients with severe multi-trauma (more than one non-head Abbreviated Injury Score >3) were excluded.

4.2 Data Sources: Patient Records

Demographic, injury, and injury scoring data; admission VS; and laboratory data are recorded by our trauma registry on all trauma patients admitted to the STC. Therapeutic interventions were abstracted from written patient charts and the electronic medical record.

4.3 High-Resolution Automated Data Collection

Vital signs data collection for this project was initiated when an ICP monitoring device was placed either in the trauma resuscitation unit or in the intensive care unit (ICU) between 2008 and 2010. Continuous, high-resolution, automated electronic VS data were collected over the course of hospitalization from severe TBI patients. A total of 207 TBI patients required ICP monitoring, of which 191 were eligible for the study, i.e., adults (>17 years old; 42 female and 149 male). Details of the electronic data capture, storage, and data point assembly procedures used in general by this study team to construct VS signal sequences for analysis have been published previously [13] and are summarized here. All ICU patient monitors at the STC capture incoming electronic data every 6 seconds. The networked ICU monitors compress the data stream and transfer it to a centralized VS data recorder server through a secured intranet. Potential artifacts and defined extreme outliers are filtered via a moving median window process.

Two types of devices are used to monitor ICP at STC. The Camino® intraparenchymal monitor (Integra LifeSciences Corp., Plainsboro, NJ) directly measures ICP in the brain parenchyma or the subarachnoid space after surgical implantation and provides continuous pressure measurements [14]. The intraventricular catheter (IVC) provides dual but not simultaneous function by both monitoring ICP and allowing drainage of cerebrospinal fluid from the ventricles; however, ICP readings are only accurate when the external drainage system is clamped. ICP clamping and measurement are performed hourly in stable patients and more often in sicker patients. In this study, we need continuous and accurate measurement at almost all time points, which only the Camino ICP monitor could provide.

4.4 Data Pre-Processing

The 6-second high-resolution electronic monitoring data contain noise, outliers, and missing values. As mentioned before, ICP can be monitored using the Camino® ICP and IVC ICP. Because of the intermittent nature of IVC ICP measurement, as well as our requirement for continuously measured ICP, we removed IVC ICP segments by reviewing all the ICP sequences with assistance of nurse records.

Using a 5-minute-long moving window, we smoothed the continuous VS waveform by averaging the values inside the window. This approach reduces the impact of noise and outliers.

Nearest neighbor regression was a special type of pre-processing that we implemented and will be discussed further in later sections. Nearest neighbor regression was used to do invariable normalization to compensate for the different ranges of the various VS variables. For example, HR usually varies from 60-120 bpm, while the SI often locates at the interval of 0 to 2. In some distance (i.e., Euclidian distance) calculations, variables with wide ranges are likely to

dominate the calculation. Small-scale variables are less important in the distance calculation. For the observations of each variable, we transformed them to be zero-mean with a covariance of one, so that all variables are in the range of -1 to 1.

4.5 Time Series Analysis of ICP

To estimate or predict ICP, we must first examine the correlation of ICP data sequence data to current and past values of the other VS. We can view the sequentially collected ICP and VS as samples from random variables that are manipulated by some underlying systems. Using auto-correlation and cross-correlation tools with the time series analysis, we can measure the linear predictability of a time point [15], i.e., if a sequence of observation is simply generated from a random process and if a linear model is sufficient to estimate and predict the variable being observed. In addition to auto-correlation and cross-correlation, which measure the linear predictability of one time series using its past or another time series, there are correlations to measure the functional dependency between variables. The maximum information coefficient (MIC) is a new measure to assess a wide range of correlations between two variables.

4.5.1 Auto-Correlation Study. Using past ICP measurements, we can predict future ICP. An autoregressive model can establish a linear function to estimate current ICP using past ICPs with lag t from a sequence of past patient ICP measurements. Knowing a reasonable duration of t could help us to develop a simple function in which past values have a strong influence on current ICP. Figure 2 shows the auto correlation of ICP in one patient with respect to different time lags. In the most recent 15 minutes, the auto-correlation is significantly different from zero. Figure 3 illustrates the auto-correlation of a group of 113 patients' ICP with lags from 5 minutes to 2 hours and demonstrates that the influence of past ICP varies among patients. However, most patients' ICPs do not have significant correlation to their own ICP 20 minutes in the past.

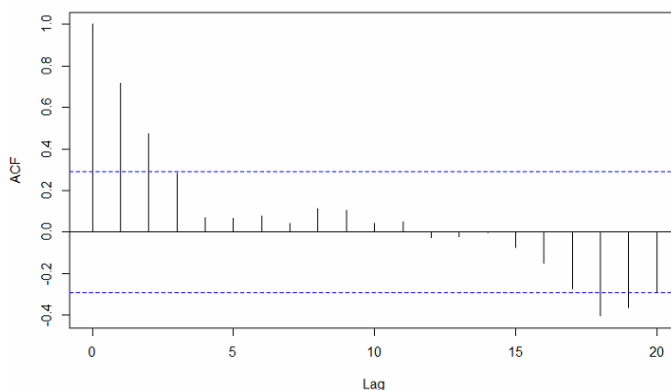


Figure 2. Auto-Correlation Function with Respect to Different Lags for One Patient's ICP

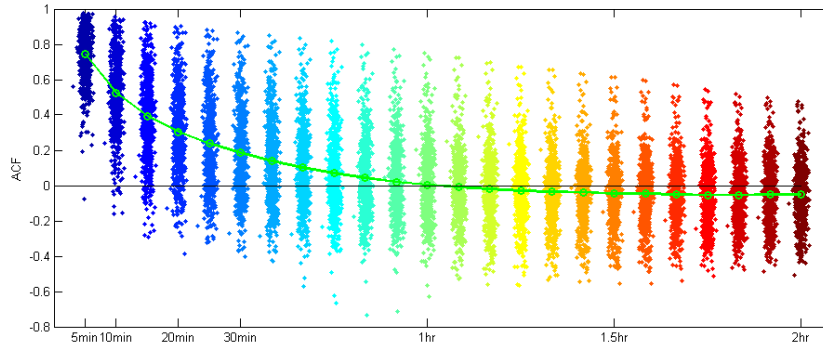


Figure 3. Jitter Plot of 113 Patients' ICP Auto-Correlation, with Maximum Lag of 2 h (24 evaluation time points with 5 min each) (most patients' ICP has little correlation after 20 min)

4.5.2 Cross-Correlation Study. To estimate ICP noninvasively from other VS readings, we needed to study how strongly ICP readings are correlated with the current and past measurements of the electronically monitored VS. Cross-correlation was used to characterize the relationship. Figure 4 shows the correlation of ICP and HR in one TBI patient with respect to different time lags. Within the past 15 minutes, the ICP is significantly correlated with patient HR.

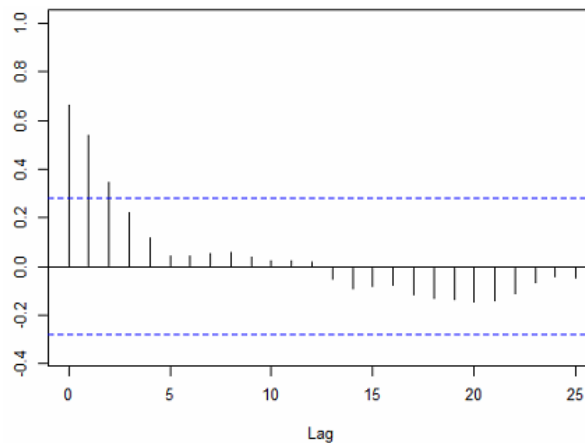


Figure 4. Cross-Correlation Function with Respect to Different Lags for One Patient's ICP and HR

4.5.3 Vital Signs Variable Dependency Test. The MIC is a new method to assess a wide range of correlations and functional dependency between two variables [16]. MIC takes real values between zero and 1, representing the non-relationship (two ends) and noise-free relationship of linear or nonlinear form, respectively. With the dataset described above, the MIC and the Pearson (linear) correlation coefficients were calculated for 15 pairs of six VS (ICP, CPP, SI, HR, SpO₂, SBP) for each patient. In Figure 5, MIC scores were plotted against Pearson coefficients to show the strength of linear and nonlinear relations. There are some interesting

observations that can be made from this plot. First, most of the VS pairs show relationships, i.e., the same color dots in the plot cluster in closed regions. Second, most pairs of variables show weak correlations, with MIC and Pearson coefficients both being close to zero. Third, both the MIC and Pearson coefficients suggest that CPP versus HR and CPP versus SpO₂ have relatively strong linear relationships. The above observations suggest that there is no simple linear relationship between ICP and other VS. Moreover, this relationship may vary between patients.

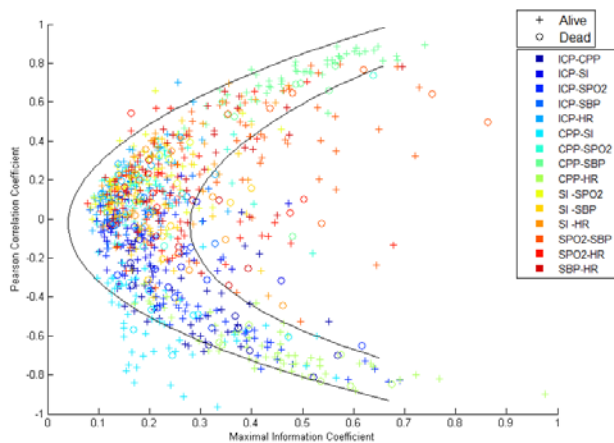


Figure 5. Pairwise Relationships of VS, Measured by MIC and Pearson's (Linear) Correlation Coefficient
(each dot represents one patient)

4.6 Estimate ICP Via Low-Rank Matrix Completion

In ICP monitoring of TBI patients, data collection is often not complete and continuous due to various technical and clinical care issues. We intend to develop machine learning algorithms that have the ability to estimate missing ICP values to ensure continuous patient care [17]. Patient data consist of continuous ICP, HR, SBP, mean blood pressure (MBP), and carbon dioxide (CO₂). Incomplete datasets are a pervasive problem in medical research. Ten patients who had 12 hours of ICP and VS without any missing ICP values and less than 5% missing values for the HR, SBP, MBP, and end tidal CO₂ (EtCO₂) were identified, only five of whom survived. We compared various methods of imputing missing data: Hankel matrix, nearest neighbor (k=1), nearest neighbor (k=5), and the regularized expectation maximization (EM) to fill in the gaps. The performance of methods was assessed and compared by comparing the relative error and the normalized mean square error (NMSE).

Traditional and intuitive methods to address estimation of missing data include filling with the mean or median [18] and/or the last observation carried forward [19]. These methods are simple but tend to give biased estimates. Moreover, they ignore information from other variables and knowledge of the system. To address these shortcomings, model-based methods have been developed, including both regression models and neural networks. These methods treat the variables with missing values in deterministic ways. However, in many applications, it makes more sense to consider variables in a probabilistic approach, as it better represents natural randomness. The maximum likelihood method such as the EM is a very successful probabilistic approach applied in missing data analysis [20,21].

Inspired by the matrix completion method [22,23], we constructed block Hankel matrices from VS data streams with missing values. We continuously estimated the missing values within a sliding window using matrix completion techniques and performed moving-window smoothing. Consider a sequence of observations $S_{t-w+1}, S_{t-w}, \dots, S_t$ for m data stream variables within a sliding window of length w that ends at time t , so that $S_i \in \mathbb{R}^m$ is the vector of values of these variables at time i . The $km \times l$ block Hankel matrix H_t at time t is constructed through a partition-and-stacking process as follows:

$$H_t = \begin{bmatrix} S_{t-w+1} & S_{t-w+2} & \dots & S_{t-w+l} \\ S_{t-w+2} & S_{t-w+3} & \dots & S_{t-w+l+1} \\ \vdots & \vdots & \vdots & \vdots \\ S_{t-w+k} & S_{t-w+k+1} & \dots & S_t \end{bmatrix},$$

where $l=w-k+1$. In constructing matrix H_t , a moving window of size w over the data stream variables is used. Within this window, the sliding sequence of length k (e.g., slices) forms the columns of H_t . Figure 6 illustrates a small example Hankel matrix constructed from 3 vital signs with a sliding window size of $w=7$ and $k=2$.

The 10 TBI patients (5 survived and 5 died in the hospital) identified above had greater than 12 hours of continuous every 6-second VS data streams without any missing ICP data and less than 5% missing values for HR, SBP, MBP, and EtCO₂. We constructed a sequence of 30×30 Hankel matrices with one matrix for each sampling step using the sliding window method. In determining the size of Hankel matrices for experiments, we tested different sizes, 15×15, 30×30, and 60×60. We chose a 30×30 Hankel matrix, as there was a noticeable improvement when going from 15 to 30 but not from 30 to 60.

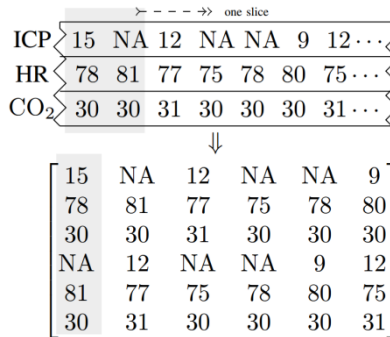


Figure 6. Example Hankel Matrix for a Sequence of m=3 VS Using a Sliding Window of Size w=7 (k=2)

We hypothesized that the vital signs would not change significantly in a short time duration and used our constructed Hankel matrices, which mostly dwell in a low dimensional space. Hence, we can find a complete matrix such that its elements are equal to the original matrix at places where there are observed values and values that have rank as small as possible at missing values. This problem can be mathematically described as a convex optimization problem and CAN be solved efficiently with off-the-shelf software.

The Hankel matrix completion method is limited by its requirement for variables to be only randomly missing and is suited for current ICP estimation, but not prediction.

4.7 ICP Prediction Via Nearest Neighbor Regression

4.7.1 Predictions with Past ICP Measurement. In this section, we will discuss the commonly used regression method to estimate and predict ICP with or without ICP measurement.

In the noninvasive ICP monitoring scenario, ICP values for training a regression model are scarce due to the relative inability to obtain ICP measurements; this absence of ICP values excludes the use of supervised learning methods. One way to resolve this sample quantity issue is to find “similar” patients whose physiological status is close to the new patient, assuming that human cerebral hemodynamics have common mechanisms between individuals, with some individual variation. This assumption would imply that two patients with similar responses to external stimulus and internal regulations should have similar trends of some physiological statuses after treatment. When matching patients with similar physiological status, there are two important challenges: (1) definition of a system state space and (2) definition of a distance metric to determine nearest neighbors of historical observation to the current conditions. After matching a set of nearest neighbors, we selected a forecast generation method, which captured the system characteristics for prediction of a short future horizon. Figure 7 depicts the idea of “borrowing” training ICP values from a historic dataset, by means of similarity.

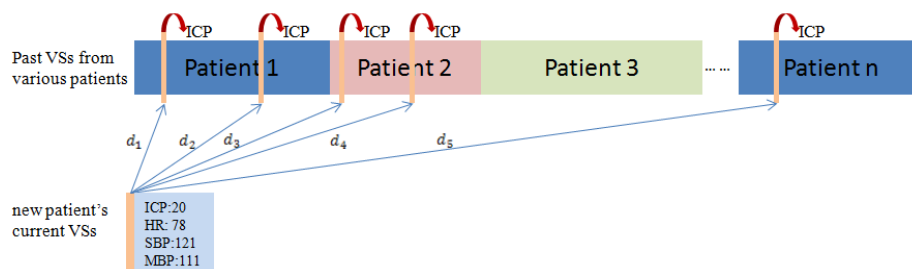


Figure 7. Illustration of Searching Nearest Neighbors Given the Current System State of a New Patient

System state similarity is measured by the distance between two system states. Hence, we need to select a set of variables to capture the characteristics of the system. In this study, we selected HR, SBP, SI, pulse pressure (PP), and ICP in the current and past 5, 10, 15, and 20 minutes. For a new patient with the above VS measured in the past 20 minutes, we search in our patient dataset for other patients to gather sufficient training points by measuring the distances between the new state and all other states. The top k nearest states (neighbors), as well their next 5-minute to 2-hour ICPs, are used as a training set to build the regression models for different prediction horizons.

After finding similar system states and their corresponding future ICP records, we used regression methods to build prediction models. Due to our limited knowledge of the physiological mechanisms by which past VS correlate with and/or influence ICP, it was difficult to design an explicit model. Therefore, instead of providing an explicit regression model with coefficients, we adopted the Gaussian process regression method to estimate the function values at each variable. This approach relaxes the parameter space into an infinite space. However,

other regression methods can also fit into this framework, such as generalized linear regression, etc.

Using the same training data found by the nearest neighbor method, we also applied the regression tree method, incorporating age, gender, and neural GCS as extra features. In most situations, the ICP changes slowly without any sharp jumps within a short time period. To some extent, the most recent ICP can be used as a rough estimation of near future ICP. To examine the performance of this simple estimation, we made shifts of ICP sequence by increasing intervals from 5 minutes up to 2 hours.

4.7.2 Predictions with Noninvasive Vital Signs Measurement. In the last section, we discussed a framework of building dynamic, local, and patient-specific models for ICP prediction using current and past invasive ICP measurements in the system state to sketch a patient's physiologic status together with other noninvasive VS. Although this setting is still useful for predicting future ICP, we hoped to make the entire process completely noninvasive. Within our framework, if we remove ICP from the system state in the similarity searching, no ICP measurement is demanded for the new patient. The only issue is that the new system state similarity between two patients may not be as good as when ICP is included. Therefore, it is necessary to select combinations of noninvasive VS that can clearly distinguish different physiologic conditions, especially the ICP. Results from this noninvasive setting are reported in the Results section below.

4.8 Evaluation of Drug Treatment and ICP Change

To improve our estimation or prediction accuracy of current and near-future ICP, we built drug treatment into our prediction models. During NTCCU care, patients receive various treatments, many of which are intended to manage ICP.

Many different sedatives, analgesics, and neuromuscular blocking agents are used to prevent, manage, and/or treat ICP elevations. Hyperosmolar agents like hypertonic saline (HTS) and mannitol are common first-line treatments for ICH. While many sedative and analgesic agents have been studied for efficacy and effect on outcome after TBI, there is little published or studied on the very short-term effects that are actually observed at the bedside and used to guide management.

We utilized high-frequency automated VS recording to examine ICP changes before and after treatment with the most commonly utilized pharmacologic interventions for ICH used at our institution. We calculated cumulative PTD ($\text{mmHg}\times\text{hr}$) and the portion of each hour spent with ICP >20 mmHg (PTI) in the hours before, during, and after intervention.

Patients with severe TBI admitted to the STC are admitted to a dedicated NTCCU and managed according to a standardized tiered protocol in accordance with the Brain Trauma Foundation Guidelines [24]. Treatment targets the maintenance of ICP <20 mmHg and CPP >60 mm Hg. We identified 98 patients out of the 191 available cases. In total, 890 treatments were administered when ICP >20 mmHg for at least 5 minutes, per continuously recorded ICP. These include 158 "small" and 71 "large" doses of HTS, respectively, 7 doses of mannitol, 325 dose escalations of propofol, 216 of fentanyl, and 89 of both propofol and fentanyl. There were also 23 administrations of a discrete dose of a barbiturate.

ICP changes after treatment in the 1-hour to 4-hour range were compared statistically. Demographic data were summarized as percentages or means with standard deviation (SD) and

medians with interquartile range. The Student's t-test was used to compare means. A statistical mixed model was applied to PTD and PTI values after treatment administration to account for multiple sampling. Probability values for results being due to chance (p) of <0.05 were considered statistically significant.

5.0 RESULTS

5.1 Time Series Analysis

In this study, we analyzed the correlation or dependency between current ICP measurements and past ICP or other VS measurements. Auto-correlation analysis for ICP shows two major observations: (1) adjacent ICPs have high correlation, but their correlation generally drops below 0.2 after 15 to 20 minutes (Figure 2), and (2) different patients presented various correlations of their current ICP to ICP in the past (Figure3). In studying correlation of ICP with another vital sign, we found similar results for ICP correlation with other VS. Based on this auto-correlation and cross-correlation study, we determined that VS measurements in the previous 15 to 20 minutes may be sufficient for estimating current ICP.

5.2 Hankel Matrix Completion

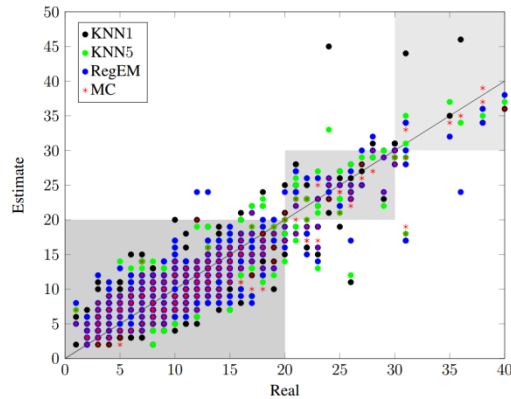
Ten patients were identified who had 12 hours of continuous (every 6 seconds) ICP and VS without any missing ICP values and less than 5% missing values for HR, SBP, MBP, and EtCO₂; five survived to discharge. Note that there are five variables in our data stream. We constructed a sequence of 30×30 Hankel matrices, one matrix for each sampling step using the sliding window method discussed in the last section. Note that each Hankel matrix contains data spanning about 3 minutes.

We use the relative error and the NMSE to assess the performance of methods in filling in missing values. The NMSE is the mean square error divided by the product of the means of the estimated value and the true value for the missing values.

In the first experiment, to represent commonly seen gaps in clinical data collection, 25% of ICP data points were randomly deleted, while leaving the VS data intact. A sequence of 30×30 Hankel matrices was constructed to estimate all missing values. If one missing ICP value appears multiple times in the same Hankel matrix, its final estimated value is calculated as the arithmetic average of all its occurrences.

Figure 8 shows a scatter plot of the true vs. the estimated value obtained from the four different fill-in methods (Hankel matrix, nearest neighbor (k=1), nearest neighbor (k=5), and the regularized EM) [25]. Points closer to the $y=x$ line indicate a smaller difference between estimated and true values. The estimates of our Hankel matrix approach (red stars) are more accurate than those of the other methods. Next, we partitioned the range of ICP values into three intervals of clinical importance: ICP values less than 20 mmHg (normal), ICP between 20 and 30 mmHg (high pressure), and ICP greater than 30 mmHg (potentially lethal; requires prompt corrective action). Clinical protocols for TBI aim to keep ICP <20 mmHg by medical interventions as necessary. Figure 9 shows that our method still performs better than other methods even for those rare instances of high ICP values. With these experiment results, we demonstrated that a few singular values are sufficient to capture most of the nuclear norm of Hankel matrices, which suggests that they are low-rank matrices perturbed with high-rank noise.

We compared our approach with commonly used data imputation methods, k-nearest neighbors (k=1, 5) and the regularized EM method, and demonstrated that our approach provides better estimates of missing values for important VS variables like ICP than these other methods.

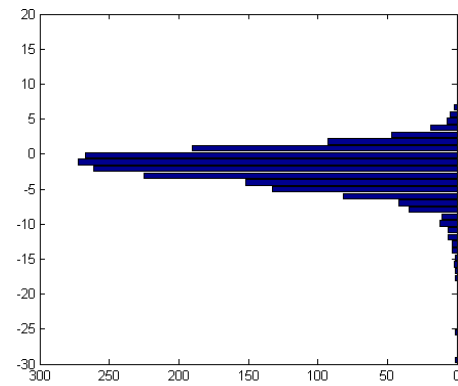
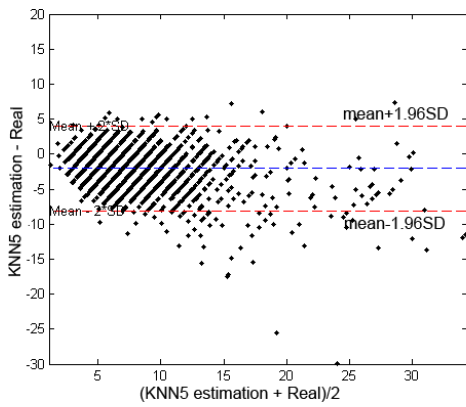
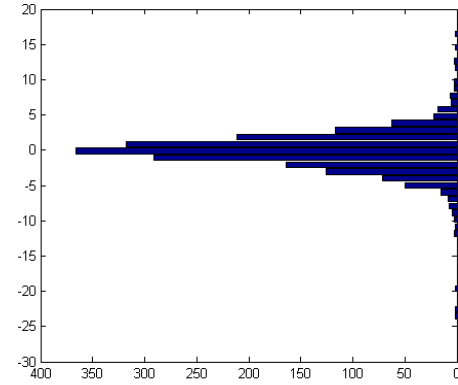
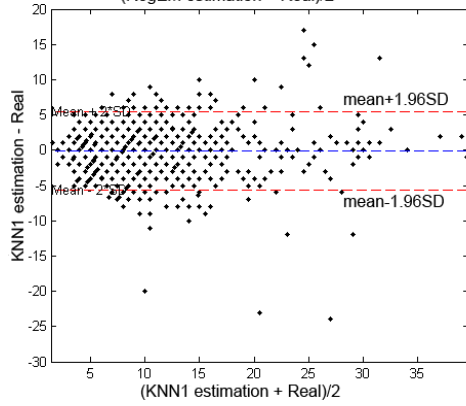
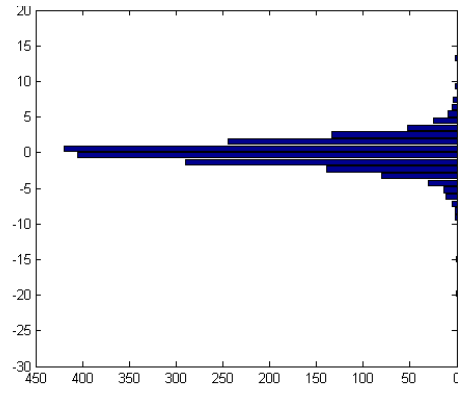
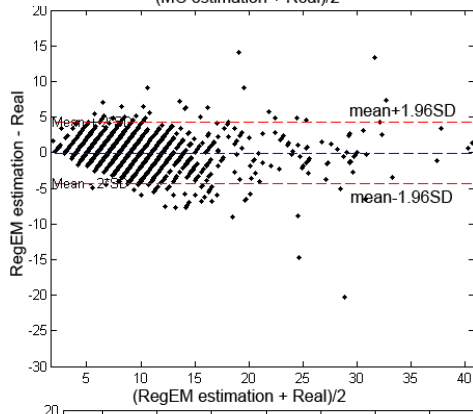
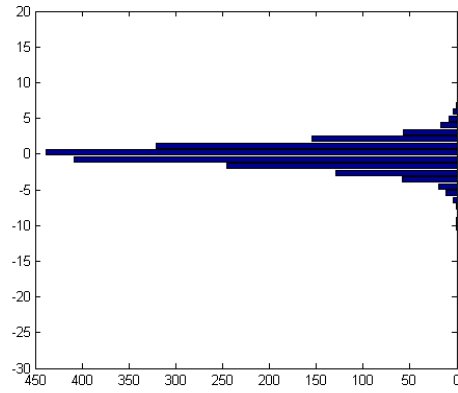
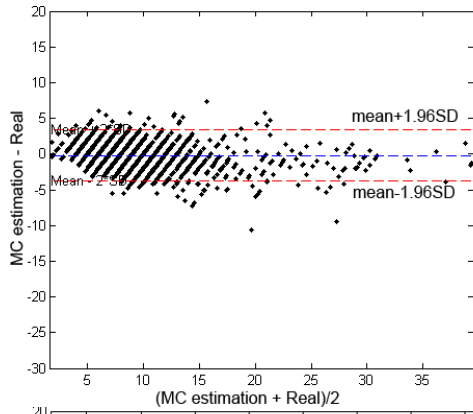


5.3 Prediction with Nearest Neighbor Regression

We evaluated our method of ICP prediction with the nearest neighbor regression (NNR) method. We compared NNR performance at ICP prediction with the regression tree method and a simple estimation way using the most recent ICP measurements using Bland-Altman plots to evaluate the agreement between the estimated values and the observed ICP sequence.

We identified a subset of 132 adult patients from the larger dataset of 191 adult patients. Continuous, automated VS data were available. All patients had severe TBI requiring the placement of a clinically necessary intraparenchymal ICP monitor (Camino). The mean age for the study group was 40.2 (SD=18.9). Patients were predominantly male (104/132). Most patients (103/132) had GCS scores of <9, the threshold often used to define severe TBI. ICP, HR, SBP, MAP, and PP were available at 5-minute temporal resolution continuously for >3 hours. This pool provided 65,600 data points, the equivalent of 5,466 hours and 40 minutes of VS monitoring. The prediction horizon ranged from 5 minutes to 2 hours. Two machine learning methods were used to create prediction models: NNR and regression tree. In training the models, only past and present VS measurements were used. The predicted ICP values then were compared against measurements for evaluation.

We applied the NNR method to predict ICP values over the next 2 hours, in sequential 5-minute segments. When we predicted ICP values for a patient, we assumed that all the rest of the patient's data were available. From the VS time series, data segments with continuous ICP, HR, SBP, PP, HR volatility, PP volatility, and MAP measurements available for more than 3 hours were used. We calculated similarity during each 30-minute period.



The Bland-Altman plots in Figure 10 show agreement between measured and predicted ICP at 5-minute, 1-hour, and 2-hour prediction horizons in the Gaussian process regression. Figure 11 compares the 1.96 SD and mean of predicted values against the measurement from the Bland-Altman plots of the NNR (red curves), the regression tree (blue curves), as well as the simple shifting estimation (green curves).

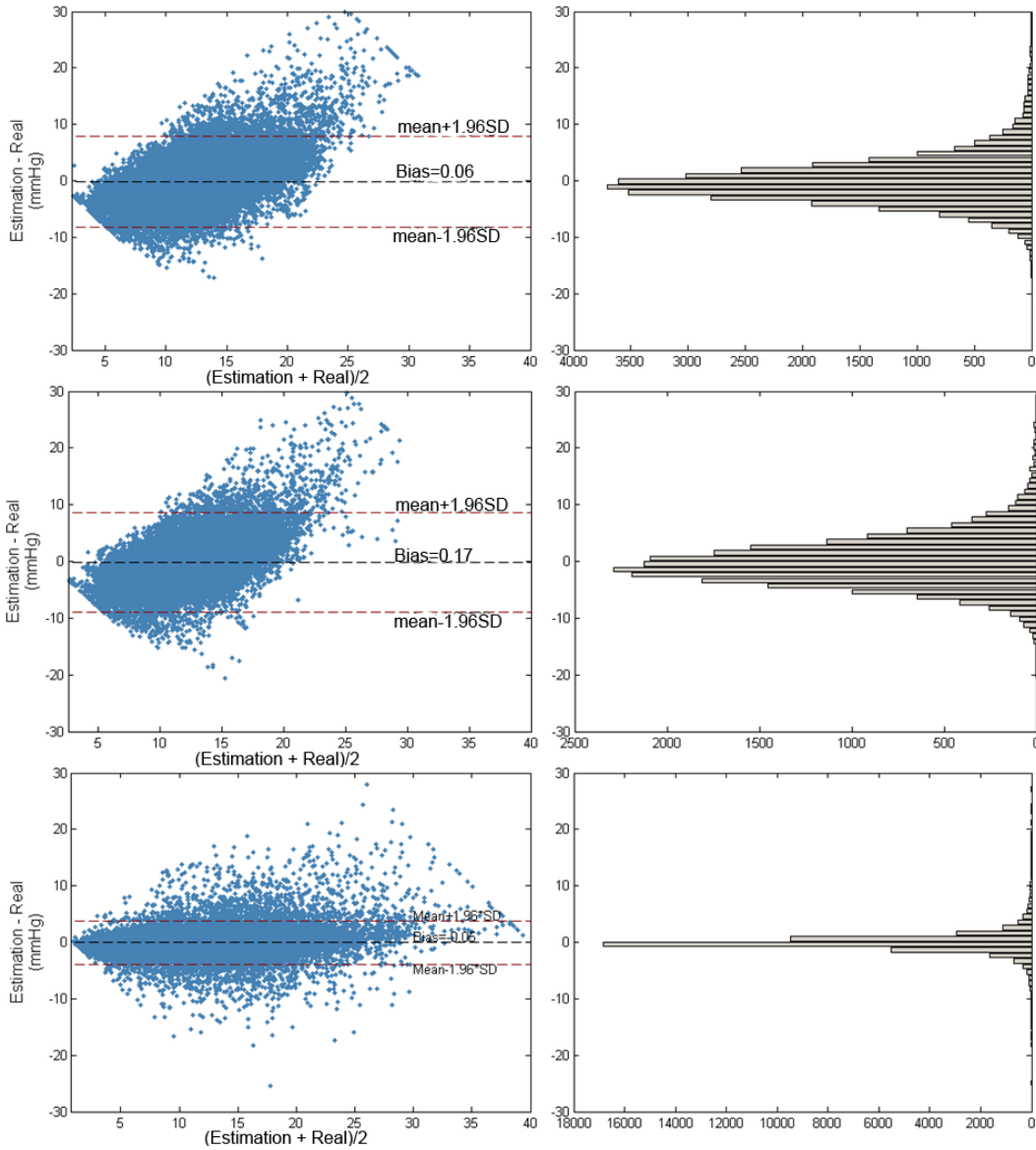


Figure 10. Performance of Comparison of Prediction for Different Prediction Horizons (5 min, 1 h, and 2 h) of the NNR Using Past ICP

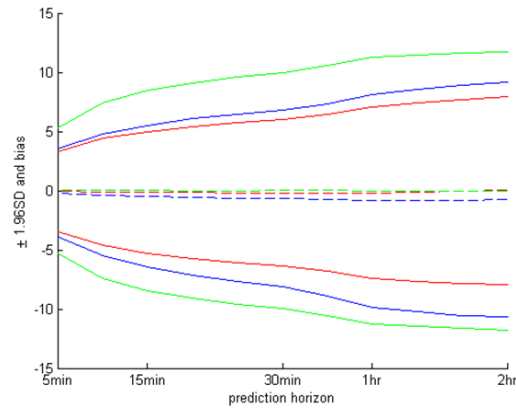


Figure 11. 1.96 SD and Bias of ICP Predictions of NNR, Regression Tree, and Most Recent ICP Carry-On

In the absence of ICP monitoring data for a patient, the real-time estimation performance of the algorithm's t (for current time) declined (bias -0.2 mmHg and SD 4.6 mmHg), when calculating the similarity between new patient and the historic dataset. This suggests that the past ICP measurement alone dominates the physiologic system state matching algorithms. In light of this, we considered another potential clinical scenario in which we have a new patient's past ICP measurement but need to stop invasive monitoring. In this case, we know the past 20 minutes of the new patient's ICP and use it to calibrate the estimation model, which has a bias of 0.002 mmHg and an SD of 1.7 mmHg, which is close to the previous result of predicting the next 5-minute ICP (SD 1.5 mmHg).

5.4 Drug Treatment and Its Impact on ICP

Various events can introduce unpredictable factors into ICP prediction. Passive manipulation of the sedated patient, such as bed transfers, can temporarily raise ICP levels. The corresponding ICP readings are real, but their significance is probably negligible. Unfortunately, such occurrences are impossible to predict and build into our machine learning models. A far more important event is clinical intervention to control elevated ICP. According to standard TBI patient management protocols, clinicians give drugs or perform other physical actions or therapies when the ICP is observed to be above certain thresholds as well as to treat other comorbidities. Any of these actions may change ICP and make ICP less predictable. Although precise prediction of the need for intervention and its potential impact is difficult, protocols calling for standard interventions under specific circumstances are available, and general predictions regarding their effects can potentially be incorporated into our models.

Ninety-eight patients met inclusion criteria [26]. Patients were primarily male (80.6%) with an average age of 39.2 ± 17.8 and a median post-resuscitation GCS score of 6; 35.7% of patients required a craniotomy for hemorrhage evacuation or a craniectomy for treatment of cerebral edema. Overall in-hospital mortality was 19.4%.

Eight hundred and ninety treatments were administered when ICP >20 mmHg for at least 5 minutes in these 98 patients. Treatments included 158 "small" and 71 "large" doses of HTS, respectively, 7 doses of mannitol, 325 dose escalations of propofol, 216 of fentanyl, and 89 of

both propofol and fentanyl. There were also 23 administrations of a discrete dose of a barbiturate.

Figure 12 shows the PTD of ICP >20 mmHg (PTD20) in the hours before, during, and after treatment administration. Values from 1-4 hours after administration reflect a statistical mixed model to account for the effect of multiple sampling in some patients. PTD20 values in the hour of treatment administration with both dose sizes of HTS, propofol, fentanyl, and propofol+fentanyl were statistically the same, while the baseline values for mannitol and barbiturates were approximately 5 and 2.5 times higher, respectively. A small dose of HTS reduced PTD20 by 34.0% in the first hour, but by the second hour the PTD20 was not different from baseline. A large dose of HTS reduced PTD by 56.3%, 78.6%, and 41.4% after hours one, two, and three, respectively. PTD did not change significantly after administration of propofol, fentanyl, or a combination of the two. No change was seen in PTD20 after administration of a dose of barbiturates.

The percentage of time per hour with ICP >20 mmHg (PTI20) before and after treatment can be seen in Figure 13. During the hour of treatment, patients spent an average of 33.6% (before fentanyl) to 78.0% (before mannitol) of the hour with ICP >20 mmHg. Baseline PTI20 was statistically comparable before administration of HTS, propofol, fentanyl, or propofol and fentanyl, while patients receiving barbiturates or mannitol showed significantly higher values. PTI20 was 36.5% lower 1 hour after a small dose of HTS and remained 30.8% lower than baseline at 2 hours. PTI20 decreased by 36.8% and 83.0% 1 or 2 hours after administration of a large dose of HTS, respectively. PTI20 remained significantly depressed for 4 hours after administration of either dose of HTS. As seen in Figure 13, PTI showed modest but significant reductions after treatment with propofol or fentanyl. There were no significant changes after treatment with mannitol or a barbiturate.

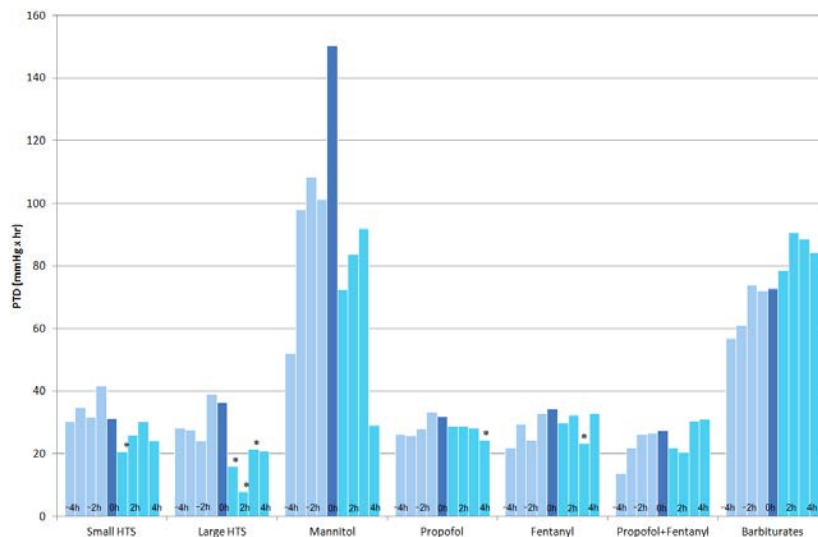


Figure 12. PTD20 in the Hours Before, During, and After Treatment Administration for Different Types of Drugs (asterisk over the bar means it has significant difference to the baseline)

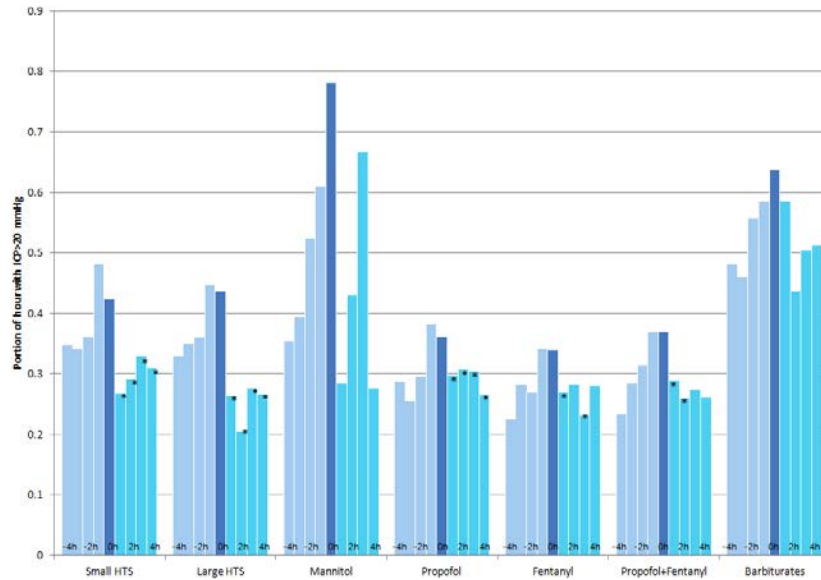


Figure 13. PTI20 in the Hours Before, During, and After Treatment Administration for Different Types of Drugs (*asterisk over the bar means it has significant difference to the baseline*)

6.0 DISCUSSION

The work described here demonstrated a framework of machine learning techniques aimed at estimating and predicting ICP, which is of great clinical importance. Intracranial pressure is the critical nexus of diagnostics, monitoring, clinical decision-making, and therapeutics for severe TBI, but current ICP monitoring instrumentation is highly invasive, fragile, difficult to use, and completely unsuitable to pre-advanced care or transport use. If successful and successfully translated into field-ready instrumentation, the work proposed here will provide clinicians with an important new, noninvasive tool for assessing ICP and critical changes in ICP over time. There is no generally accepted and widely used noninvasive ICP monitoring technique.

In this work, we experimentally showed how noninvasive monitoring of routine patient vital signs could help to estimate and predict ICP in patients with severe TBI. First, we used methods from time series analysis to study the correlation and dependency of ICP on its past or on other noninvasive vital signs. Second, under different assumptions on past ICP availability, we proposed a Hankel matrix completion method to estimate missing ICP measurements by sequentially solving an optimization problem. This method has proven useful when we need to impute missing ICP during continuous ICP monitoring of a patient with TBI. To implement completely noninvasive ICP monitoring, we created a historic dataset with invasive ICP measured from 191 other patients. With noninvasive vital signs measured for a new patient, we matched physiologic similar system states from the dataset and pulled out a subset of ICP values that are likely to be the ICP value if the similar physiologic system state is observed.

As a framework, the nearest neighbor method is flexible enough to include new information, such as a new vital sign that can better approximate the physiologic similarity. It can also make use of patients' past ICP measurements, if available. This method could eventually provide ICP estimation completely noninvasively for new patients. In the meantime, it can be used to build patient-specific models that are adaptive to new physiologic changes as they occur. We suggest that the noninvasive ICP estimation with nearest neighbor regression would be particularly helpful if we have a short duration (20 minutes) of ICP measurement to calibrate our algorithm.

Clinical interventions often have significant impact on vital signs or ICP trajectory. In the drug treatment study, we identified a set of drugs commonly used in ICP management that have statistical significance in changing ICP for up to 4 hours after administration. If the estimation model can incorporate drug treatment given a few hours previously, the estimation of current ICP could be adjusted and be more accurate.

7.0 CONCLUSIONS

With exploratory time series analysis and experiments, we found that noninvasive vital signs potentially can be used to estimate current ICP values or predict near-future ICP values. The estimation and prediction framework described above allows us to use a historic patient dataset with ICP monitoring to develop an algorithm that can complete noninvasive ICP monitoring for new patients. The framework is flexible to incorporate new variables that are strongly correlated to ICP and hence improve the accuracy and can run on field-deployable devices to provide real-time ICP estimation and decision support software, given other noninvasive vital signs.

7.1 Immediate Impact

The noninvasive ICP monitoring framework can be applied to our additional projects funded by or in consideration by the U.S. Air Force. "Fit to Fly" (FA8650-12-2-6D09) examines the correlation between biomarker cytokines and adverse ICP or ICH-related events in 6- to 12-hour intervals from the time of TBI patient admission through the first 72 hours. Noninvasive ICP monitoring can be used during the transportation of patients or as a decision assist method for determining when to transfer a patient. "A Prospective Study of the Use of First 12-hour Intracranial Pressure Data to Provide Long-Term Prognosis after Severe Traumatic Brain Injury" is currently under review at the 711th Human Performance Wing. This pre-proposal proposes to test the algorithms developed in the current work against a prospective, novel dataset.

7.2 Cost and Ease of Use

The noninvasive ICP monitoring framework proposed in this study relies on automated, continuous (noninvasive) vital signs monitoring and on an existing high-quality historic dataset that can represent relationships between ICP and other vital signs. These are commonly available in modern neurocritical care units. These algorithms can run on mainstream computers or could be optimized for running efficiency and embedded into industrial vital signs monitoring devices.

This framework does not require probe devices beyond those used in routine care. It displays the ICP estimations. However, the algorithms may also provide confidence intervals to show the uncertainty of the estimation or prediction, which may add extra information to the display.

7.3 Limitations

Although this ICP monitoring framework is very flexible for estimation (current) or prediction (future), its performance is limited by some factors. First, the method depends on a historic dataset (like a dictionary), and the quality of data in that dataset has huge impact on the estimation accuracy. Second, finding a similar system state between a new patient and the dataset relies on selection of a set of relevant noninvasive vital signs. Our study shows that additional work is needed to identify a good combination of those vital signs for improved accuracy. Third, as we discussed above, intervention information may help to improve estimation. However, it requires extra effort to capture the relevant intervention events and to incorporate them into the models.

8.0 REFERENCES

1. DuBose JJ, Barmparas G, Inaba K, Stein DM, Scalea T, Cancio LC, et al. Isolated severe traumatic brain injuries sustained during combat operations: demographics, mortality outcomes, and lessons to be learned from contrasts to civilian counterparts. *J Trauma* 2011; 70(1):11-6.
2. Eastridge BJ, Stansbury LG, Stinger H, Blackburne L, Holcomb JB. Forward Surgical Teams provide comparable outcomes to combat support hospitals during support and stabilization operations on the battlefield. *J Trauma* 2009; 66(4 Suppl):S48-50.
3. Vanderploeg RD, Schwab K, Walker WC, Fraser JA, Sigford BJ, Date ES, et al. Rehabilitation of traumatic brain injury in active duty military personnel and veterans: Defense and Veterans Brain Injury Center randomized controlled trial of two rehabilitation approaches. *Arch Phys Med Rehabil* 2008; 89(12):2227-38.
4. Goodman MD, Makley AT, Lentsch AB, Barnes SL, Dorlac GR, Dorlac WC, et al. Traumatic brain injury and aeromedical evacuation: when is the brain fit to fly? *J Surg Res* 2010; 164(2):286-93.
5. Goodman MD, Makley AT, Huber NL, et al. Hypobaric hypoxia exacerbates the neuroinflammatory response to traumatic brain injury. *J Surg Res*. 2010; 165:30-37.
6. Dutton RP, Stansbury LG, Leone S, Kramer E, Hess JR, Scalea TM. Trauma mortality in mature trauma systems: are we doing better? An analysis of trauma mortality patterns, 1997-2008. *J Trauma* 2010; 69(3):620-6.
7. Eastridge BJ, Mabry RL, Seguin P, Cantrell J, Tops T, Uribe P, et al. Death on the battlefield (2001-2011): implications for the future of combat casualty care. *J Trauma Acute Care Surg* 2012; 73(6 Suppl 5):S431-7.
8. Stein DM, Hu PF, Brenner M, Sheth KN, Liu KH, Xiong W, et al. Brief episodes of intracranial hypertension and cerebral hypoperfusion are associated with poor functional outcome after severe traumatic brain injury. *J Trauma* 2011; 71(2):364-73.
9. Smith M. Monitoring intracranial pressure in traumatic brain injury. *Anesth Analg* 2008; 106(1):240-8.

10. Kahraman S, Dutton RP, Hu P, Xiao Y, Aarabi B, Stein DM, et al. Automatic measurement of “pressure times time dose” of intracranial hypertension best predicts outcome after severe traumatic brain injury. *J Trauma* 2010; 69(1):110-8.
11. Jennett B, Snoek J, Bond MR, Brooks N. Disability after severe head injury: observations on the use of the Glasgow Outcome Scale. *J Neurol Neurosurg Psychiatry* 1981; 44(4):285-93.
12. Kahraman S, Hu P, Stein DM, Stansbury LG, Dutton RP, Xiao Y, et al. Dynamic three-dimensional scoring of cerebral perfusion pressure and intracranial pressure provides a brain trauma index that predicts outcome in patients with severe traumatic brain injury. *J Trauma* 2011; 70(3):547-53.
13. Kahraman S, Dutton RP, Hu P, Stansbury L, Xiao Y, Stein DM, et al. Heart rate and pulse pressure variability are associated with intractable intracranial hypertension after severe traumatic brain injury. *J Neurosurg Anesthesiol* 2010; 22(4):296-302.
14. Pattinson K, Wynne-Jones G, Imray CH. Monitoring intracranial pressure, perfusion and metabolism. *Continuing Education in Anaesthesia, Critical Care and Pain* 2005; 5:130-3.
15. Shumway RH, Stoffer DS. Time series analysis and its applications: with R examples, 3rd ed. New York: Springer; pp.17-22, 2011.
16. Reshef DN, Reshef YA, Finucane HK, Grossman SR, McVean G, Turnbaugh PJ, et al. Detecting novel associations in large data sets. *Science* 2011; 334(6062):1518-24.
17. Yang S, Kalpakis K, Mackenzie CF, Stansbury LG, Stein DM, Scalea TM., et al. Online recovery of missing values in vital signs data streams using low-rank matrix completion. 11th International Conference on Machine Learning and Applications (ICMLA) 2012; 1:281-7.
18. Daniels MJ, Hogan JW. Missing data in longitudinal studies: strategies for Bayesian modeling and sensitivity analysis. Boca Raton, FL: Chapman & Hall/CRC; pp.42, 2008.
19. Haukoos JS, Newgard CD. Advanced statistics: missing data in clinical research—part 1: an introduction and conceptual framework. *Acad Emerg Med* 2007; 14(7):662-8.
20. Enders CK. Applied missing data analysis. New York: The Guilford Press; pp.103-5, 2010.
21. Nelwamondo FV, Mohamed S, Marwala T. Missing data: a comparison of neural network and expectation maximisation techniques. arXiv:0704.3474v1; 2007. Retrieved 1 November 2013 from <http://arxiv.org/ftp/arxiv/papers/0704/0704.3474.pdf>.
22. Candès EJ, Recht B. Exact matrix completion via convex optimization. *Found Comput Math* 2009; 9:717-72.
23. Candès EJ, Plan Y. Matrix completion with noise. *Proceedings of the IEEE* 2010; 98(6):925-36.
24. Brain Trauma Foundation, American Association of Neurological Surgeons, Congress of Neurological Surgeons. Guidelines for the management of severe traumatic brain injury. *J Neurotrauma* 2007; 24 Suppl 1:S1-106.
25. Li H, Zhang K, Jiang T. The regularized EM algorithm. *Proceedings of the 20th National Conference on Artificial Intelligence*; 2005 Jul 9-13; Pittsburgh, PA. Menlo Park, CA: AAAI Press; 2005:807-12.
26. Colton K, Yang S, Hu P, Chen H, Stansbury L, Scalea T, et al. Intracranial pressure response after pharmacologic treatment of intracranial hypertension. Abstract presented at the 27th Eastern Association for the Surgery of Trauma (EAST) Annual Scientific Assembly; 2014 Jan 14-18; Naples, FL.

LIST OF ABBREVIATIONS AND ACRONYMS

BTI	Brain Trauma Index
CO₂	carbon dioxide
CPP	cerebral perfusion pressure
EM	expectation maximization
EtCO₂	end tidal carbon dioxide
GCS	Glasgow Coma Scale
HR	heart rate
HTS	hypertonic saline
ICH	intracranial hypertension
ICP	intracranial pressure
ICU	intensive care unit
IVC	intraventricular catheter
MAP	mean arterial pressure
MBP	mean blood pressure
MIC	maximum information coefficient
NMSE	normalized mean square error
NNR	nearest neighbor regression
NTCCU	neurotrauma critical care unit
PP	pulse pressure
PTD	pressure-times-time dose
PTI	portion of each hour spent with ICP >20 mmHg
SD	standard deviation
SpO₂	oxygen saturation
SBP	systolic blood pressure
SI	Shock Index
STC	R Adams Cowley Shock Trauma Center
TBI	traumatic brain injury
VS	vital signs